Geomagnetically trapped and albedo protons measured by PAMELA

Alessandro Bruno

Università degli Studi di Bari, Italy

on behalf of the PAMELA collaboration

Space Radiation and Plasma Monitoring Workshop, 13-14 May 2014
European Space Research and Technology Centre (ESTEC)

Outline

- Brief description of the PAMELA experiment and data analysis

- PAMELA results
  1) geomagnetically trapped protons
  2) (re-entrant) albedo protons

- Conclusions

The PAMELA collaboration

Italy:

Bari | Florence | Frascati | Naples | Rome | Trieste | CNR, Florence

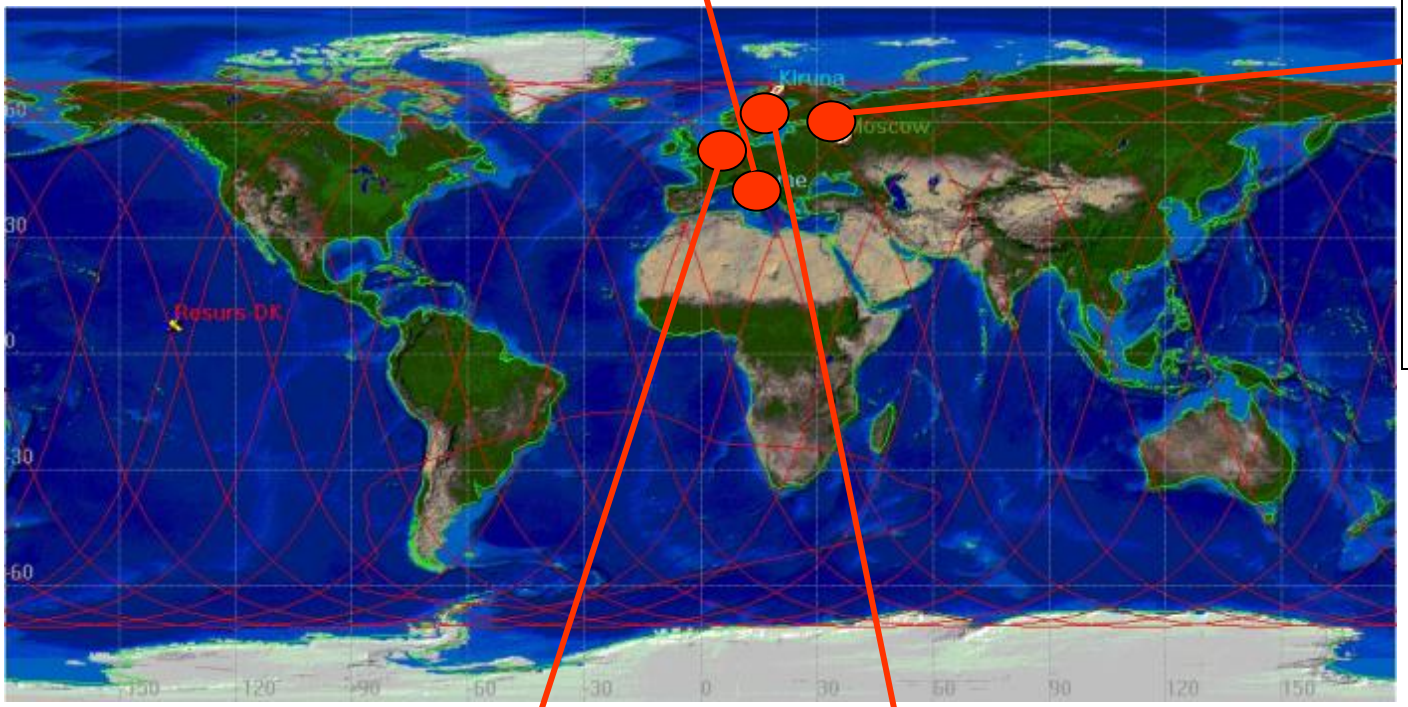

Russia:

Moscow
St. Petersburg

Germany: Siegen

Sweden: KTH, Stockholm

The PAMELA apparatus

Main requirements → high-sensitivity particle identification and precise momentum measure

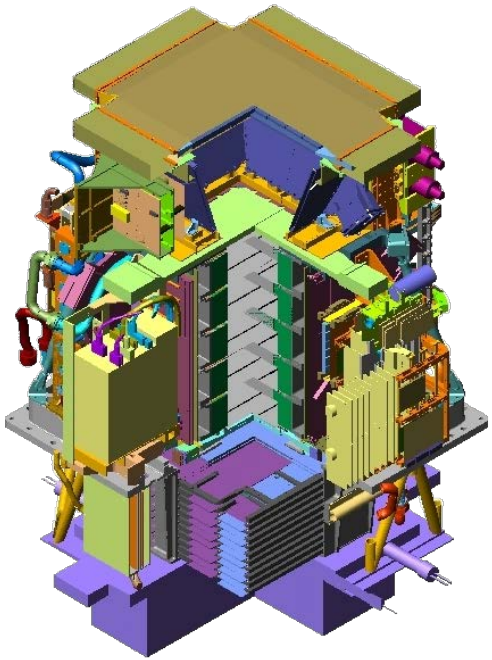

Size: 130x70x70 cm^3
GF: 21.5 cm^2 sr
Mass: 470 kg
Power Budget: 360W

Time-Of-Flight
plastic scintillators + PMT
- Trigger
- Albedo rejection;
- Mass identification up to 1 GeV;
- Charge identification from dE/dX.
-

Anticoincidence shield
plastic scintillators + PMT

Electromagnetic calorimeter
W/Si sampling (16.3 X_0, 0.6 λI)
- Discrimination e+ / p, anti-p / e^- (shower topology)
- Direct E measurement for e^-

Bottom scintillator (+PMT)

Neutron detector
^{3}He counters
- High-energy e/h discrimination

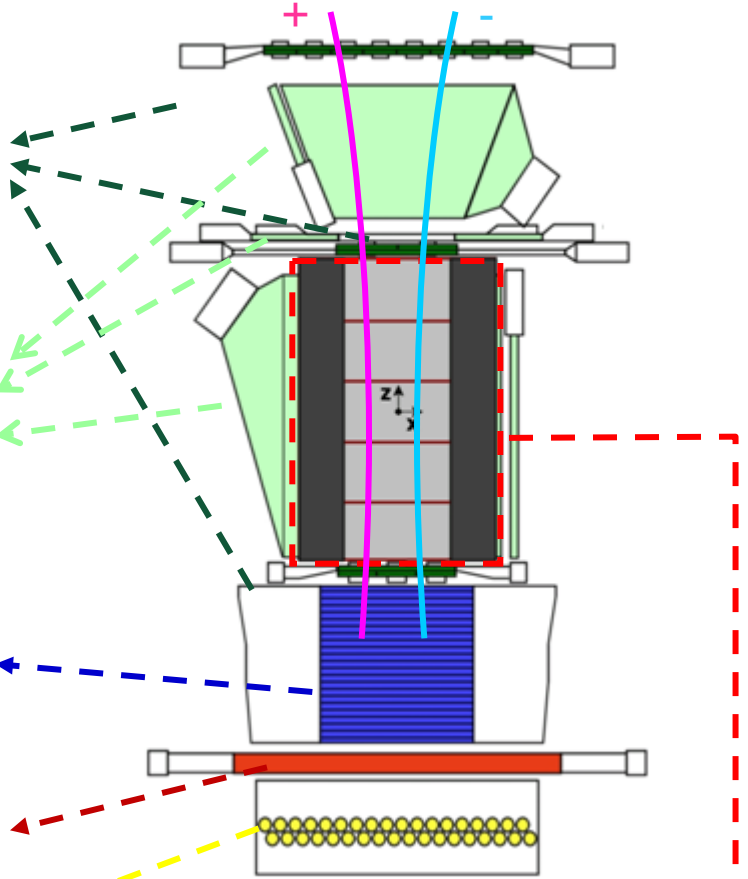

Spectrometer
microstrip silicon tracking system + permanent magnet
- Magnetic rigidity: R=pc/Ze
- Charge sign
- Charge value from dE/dx

The Resurs-DK1 satellite

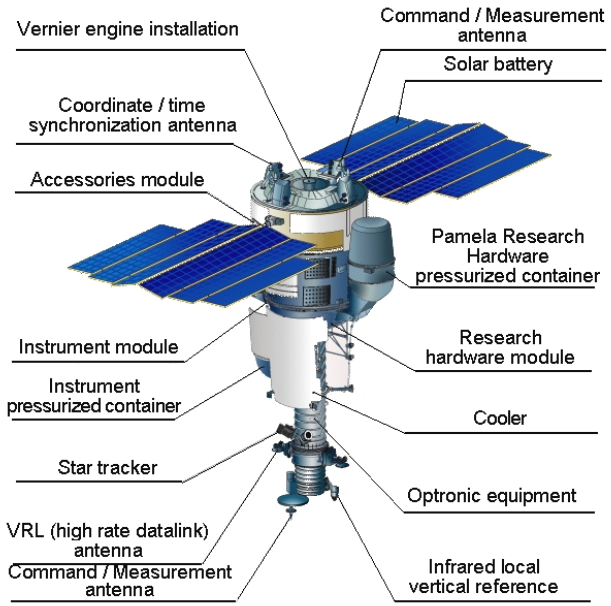

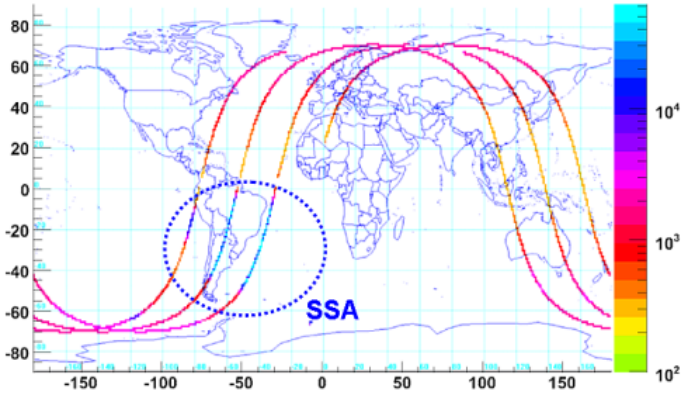

- Mass: ~6.7 tons
- Height: 7.4 m
- Solar array span: ~14 m
- Average power (per day): 2000 W (PAMELA 360 W)

- Semi-polar (70° inclination) and elliptical (350÷610 km altitude) orbit
- Orbital period: 96 minutes

- 3-axis stabilized
- Orientation calculated by onboard processor with accuracy <1°
- Angular velocity stabilization accuracy: 0.005 degree/s

➢ In orbit since June 15th 2006

Data analysis

- Data recorded by PAMELA between **July 2006 and September 2009**

  - McIlwain's coordinates and other magnetic variables of interest (e.g. the adiabatic invariants), calculated on an event-by-event basis using the **IRBEM** library (Boscher et al. 2012).

  - **Realistic description of the Earth's magnetosphere**
    - internal geomagnetic field: IGRF-10 (Macmillan & Maus 2010)
    - external geomagnetic field: TS05 (Tsyganenko & Sitnov 2005)
      - dynamical model of the storm-time geomagnetic field in the inner magnetosphere, based on recent space magnetometer data and concurrent observations of the solar wind and IMF.

- Proton trajectories reconstructed in the Earth's magnetosphere using a **tracing program** based on numerical integration methods (Smart & Shea 2000, 2005), and implementing the afore-mentioned models.

  Trajectories propagated back and forth from the measurement location, and followed until:

interplanetary →
re-entrant albedo →
geomagnetically stably-trapped →

1) they escape model magnetosphere boundaries;
2) or they intersected the absorbing atmosphere limit, which was assumed at an altitude of 40 km (mean proton production altitude);
3) or they performed more than 3×10^6/R steps (R=particle rigidity in GV) for both propagation directions.
   - ✓ step-length ~1% of a particle gyro-distance in the magnetic field

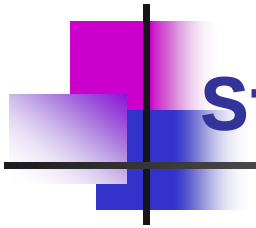

Stably-trapped protons

Data analysis

- Data were analyzed in the framework of the **adiabatic theory**
  - relatively simple description of the complex dynamics of charged particles in the magnetosphere.

- The motion of trapped particles was assumed to be a superposition of 3 periodic motions:
  1) a **gyration** around the local magnetic field lines,
  2) a **bouncing** along field lines between conjugate mirror points in the northern and southern hemispheres,
  3) and a slow **drift** around the Earth.

- Each kind of motion is related to an **adiabatic invariant**
  - conserved under the condition of small magnetic field variations during the period of the motion, and in absence of energy loss, nuclear scattering and radial diffusion.

- Geomagnetic selection: only protons with rigidity $R < 10 / L^3$ GV (L = McIlwain's parameter);
  - to reject eject events near the local geomagnetic cutoff (chaotic trajectories of non-adiabatic type)

Back-tracing and particle classification

For each event, the number of gyrations, bounces and drifts was evaluated in order to estimate corresponding frequencies and check trajectory behaviors.

By using combined selections on corresponding mean frequencies ω_i (i =gyro, bounce, drift) as a function of several variables of interest (E, α, Λ, etc.), the analyzed sample was sub-divided into three categories:

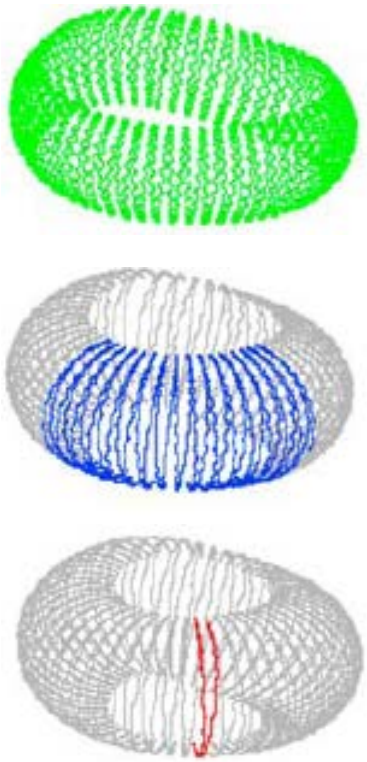

- **stably-trapped** protons perform several drift cycles (>4) around the Earth without intercepting the absorbing atmosphere limit.
  - They satisfy adiabatic conditions: $\omega_{bounce}/\omega_{gyro} \leq 0.3$ and $\omega_{drift}/\omega_{bounce} \leq 0.01$
  - NB: the tracing technique allowed to account for the breakdown of trapping at high energies, as consequence of either large gyro-radius or non-adiabatic trajectory effects
- **quasi-trapped** protons:
  - trajectories similar to those of stably-trapped protons, but are originated and re-absorbed by the atmosphere during a time larger than a bounce period.
  - Their trajectories were verified to satisfy the adiabatic conditions, in particular the hierarchy of temporal scales: $\omega_{bounce}/\omega_{gyro} \leq 0.3$ and $\omega_{drift}/\omega_{bounce} \leq 0.03$
- **un-trapped** protons:
  - originated and absorbed absorbed by the atmosphere within a bounce period.

PAMELA directional response

- **Gathering power** [cm^{2}sr] (Sullivan 1971):

$$\Gamma = \int_{\Omega} d\omega F(\omega) \int_{S} \mathrm{d}\sigma \cdot \hat{\mathrm{r}} = \int_{\Omega} d\omega F(\omega) \mathrm{A}(\omega)$$

where F(ω) represents the angular dependence of the incident flux (F(ω)=1 for isotropic exposition) and A(ω) is the detector response function

  - Due to the bending effect of the magnetic spectrometer, PAMELA gathering power depends also on particle rigidity: $\Gamma = \Gamma(R)$

- **SAA**: strong anisotropy due to the interaction with the atmosphere: $0 \leq F(\omega) \leq 1$
  - The apparatus gathering power depends on spacecraft orientation with respect to the geomagnetic field direction

- **PAMELA effective area** [cm^2] evaluated as a function of satellite orientation $\Psi = (\vartheta_B, \varphi_B)$, proton local pitch angle **α** and kinetic energy **E**, and averaged over gyro-phase angle β:

$$H(\Psi,\alpha,E) = \frac{1}{2\pi} \int_{0}^{2\pi} d\beta \left[A\left(E, \vartheta(\Psi,\alpha,\beta), \varphi(\Psi,\alpha,\beta)\right) \cos\vartheta(\Psi,\alpha,\beta) \sin\alpha \right]$$

where $\vartheta = \vartheta(\Psi,\alpha,\beta)$ and $\varphi = \varphi(\Psi,\alpha,\beta)$ are the zenith and azimuth angles in the PAMELA frame

  - Accurate montecarlo calculation:
    - Satellite orientation: 360 x 180 bins (range: azimuth 0-360 deg, zenith 0-180 deg)
    - Local pitch angle: 180 bins (range: 0 to 180 deg)
    - Kinetic energy: 30 log bins (range: 63 MeV – 10 GeV)
    - Small simulation statistical uncertainty (<1%)
    - Inelastic interactions/scattering inside the apparatus accounted for

Flux mapping

1) Differential directional fluxes (GeV $^{-1}$m^{-2}s^{-1}sr^{-1}) were calculated over a 5-dimensional grid F(**X**,α,E), where **X**=(Lat, Lon, Alt) denotes the geographic position.
   - The grid extends over the whole phase-space region covered by PAMELA, for a total number of bins amounting to (n_{Lat} x n_{Lon} x n_{Alt} x n_{α} x n_{E}) = (70 x 180 x 13 x 180 x 42).

2) Guiding center correction
   - proton gyro-radius at PAMELA energies: from some tens to several hundreds km
   - in order to account for finite gyro-radius effects (East-West effect), measurements were shifted to corresponding guiding center positions $\mathbf{X_{GC}}$ = (Lat_{GC}, Lon_{GC}, Alt_{GC})

1) Then the geographic flux grid F($\mathbf{X_{GC}}$,α,E) was interpolated onto magnetic coordinates, using several invariant coordinate systems
   - Adiabatic invariants: $M = \frac{p^2}{2m_0 B_m}, \quad K = \int_{s_m}^{s'_m} \left[B_m - B(s)\right]^{1/2} ds, \quad \Phi = \oint A \cdot dl$
   - Equatorial pitch angle α_{eq} vs McIlwain's L-shell
   - Roederer L-shell: $L^* = \frac{2\pi\mu_E}{R_E \Phi}$
   - Invariant altitude vs magnetic latitude $h_{inv} = (r-1)\cdot R_E, \qquad \cos^2\lambda = r/L$

Geographic maps

stably-trapped protons

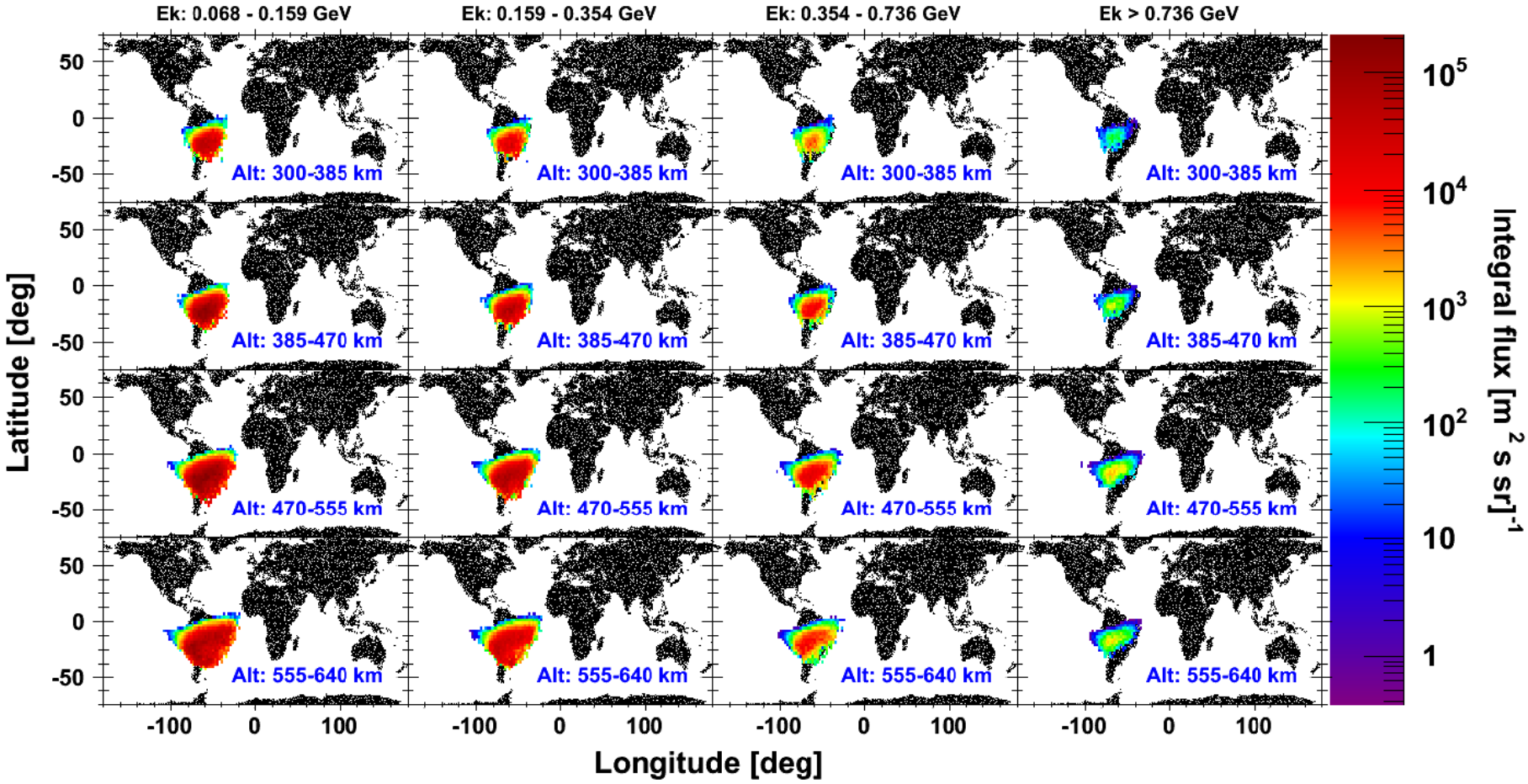

Stably-trapped integral fluxes ($m^{-2}s^{-1}sr^{-1}$) averaged over the pitch angle range covered by PAMELA, as a function of geographic coordinates, evaluated for different energy (columns) and guiding center altitude (rows) bins.

Invariant maps: Φ vs K

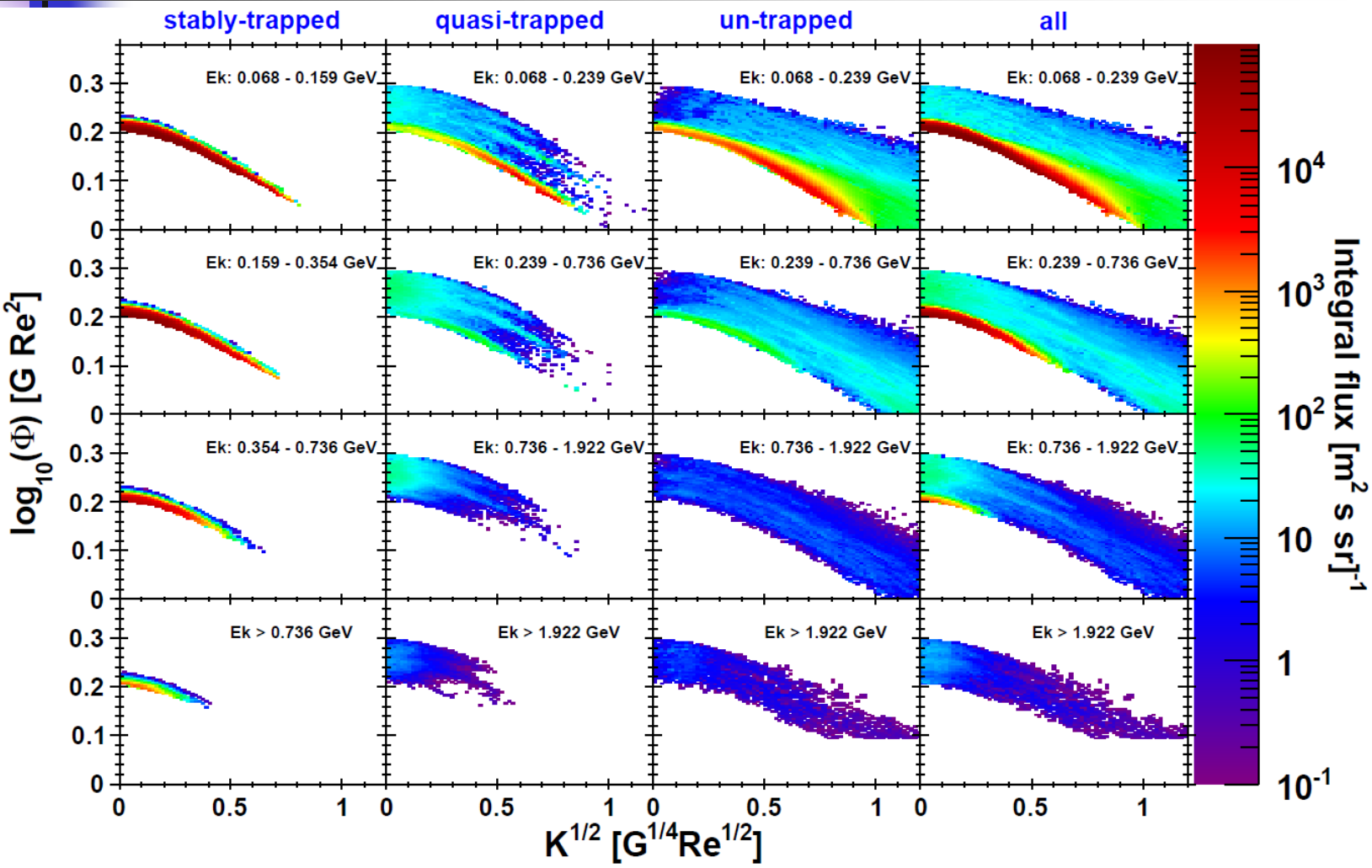

Proton integral fluxes ($m^{-2}s^{-1}sr^{-1}$) as a function of the second K and the third Φ adiabatic invariant, for different kinetic energy bins (see the labels).

Invariant maps: α_{eq} vs L

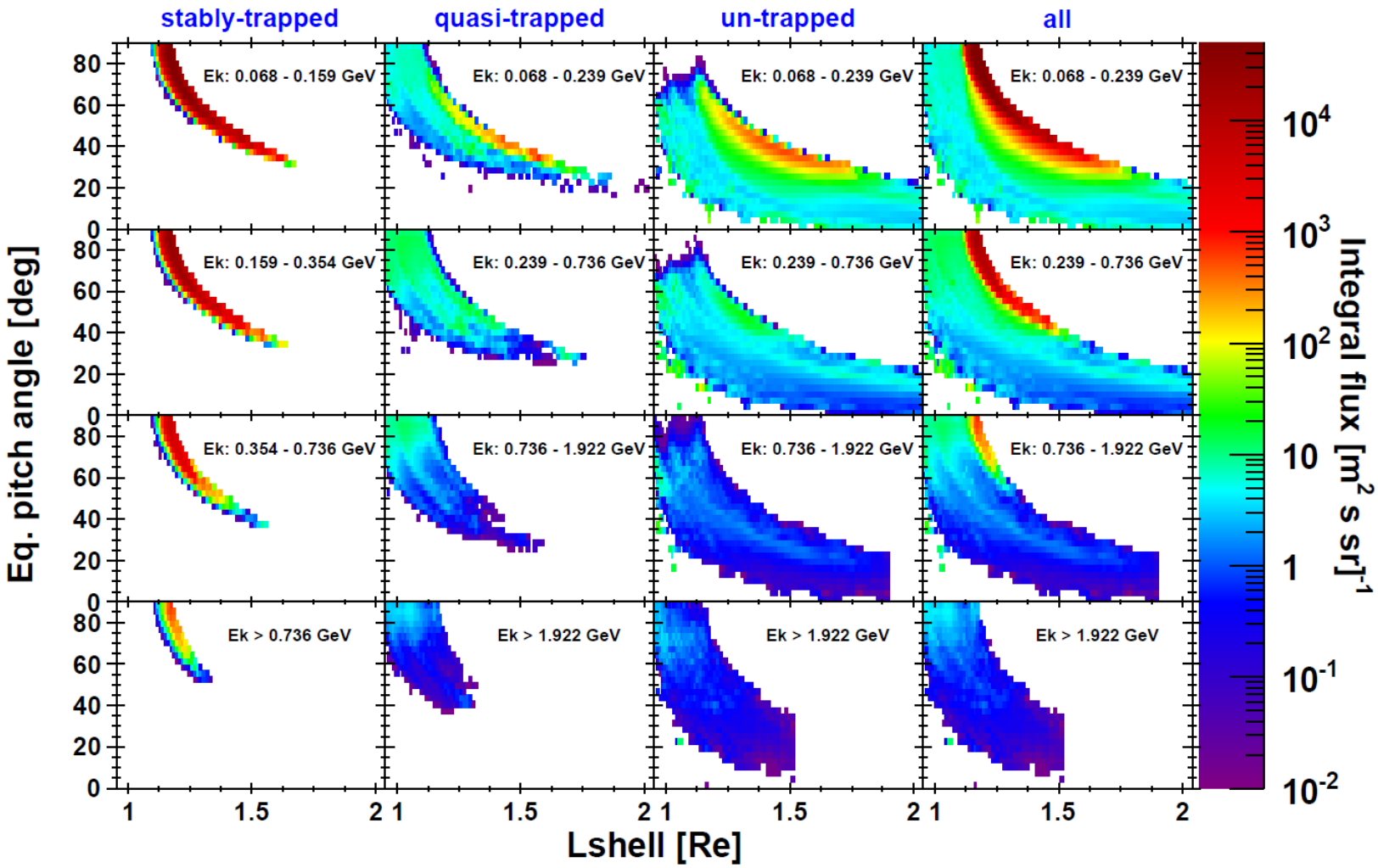

Proton integral fluxes ($m^{-2}s^{-1}sr^{-1}$) as a function of equatorial pitch angle and McIlwain's *L*-shell, for different kinetic energy bins (see the labels).

Invariant maps: h_{inv} vs λ

more adequate spatial resolution at low altitudes or near the loss cone (Cabrera & Lemaire 2007)

$$h_{inv} = (r-1)\cdot R_E, \qquad \cos^2\lambda = r/L$$

where:
L = McIlwain's L-shell
r = radiali distance in McIlwain's reference dipole

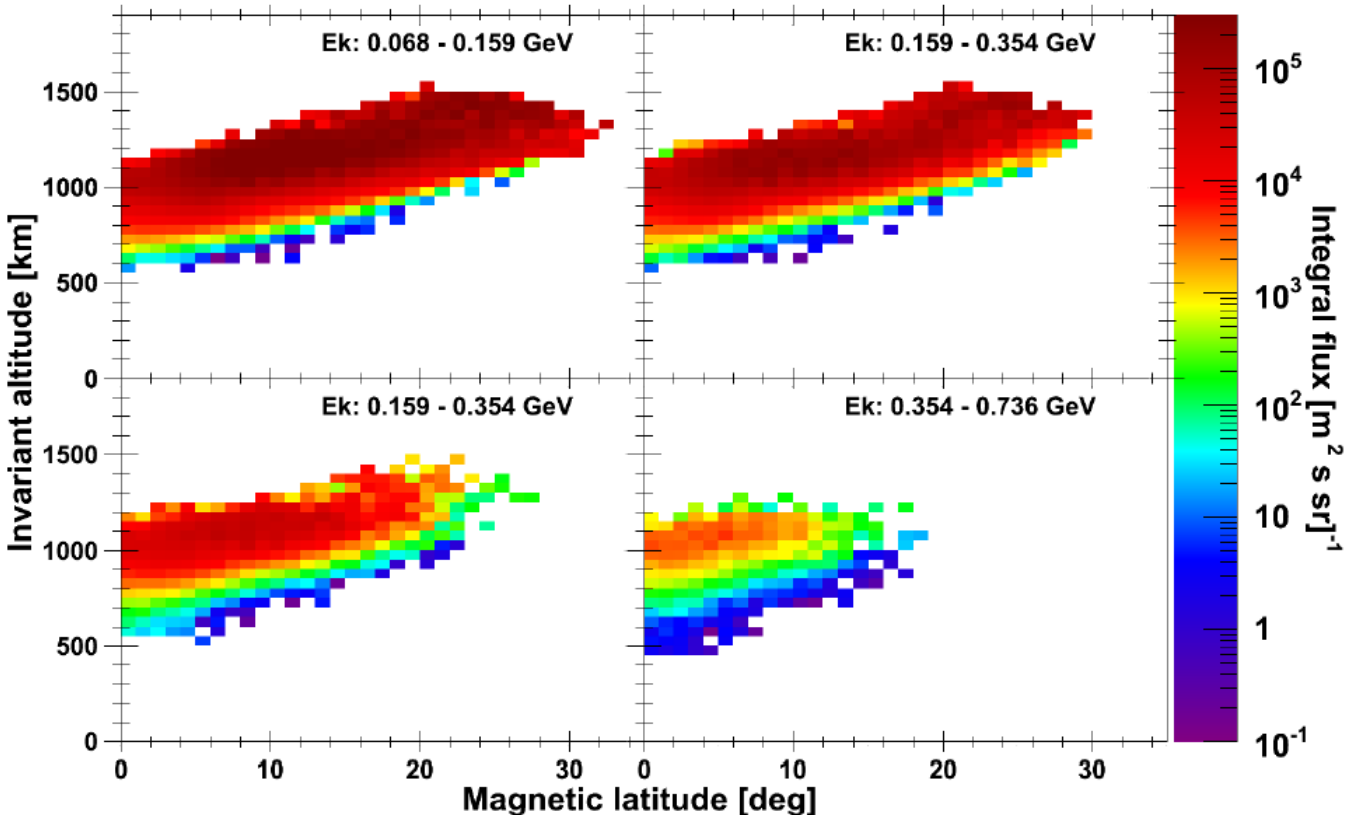

Stably-trapped integral fluxes ($m^{-2}s^{-1}sr^{-1}$) as a function of magnetic latitude and invariant altitude, for different energy bins.

Comparison with emphirical models

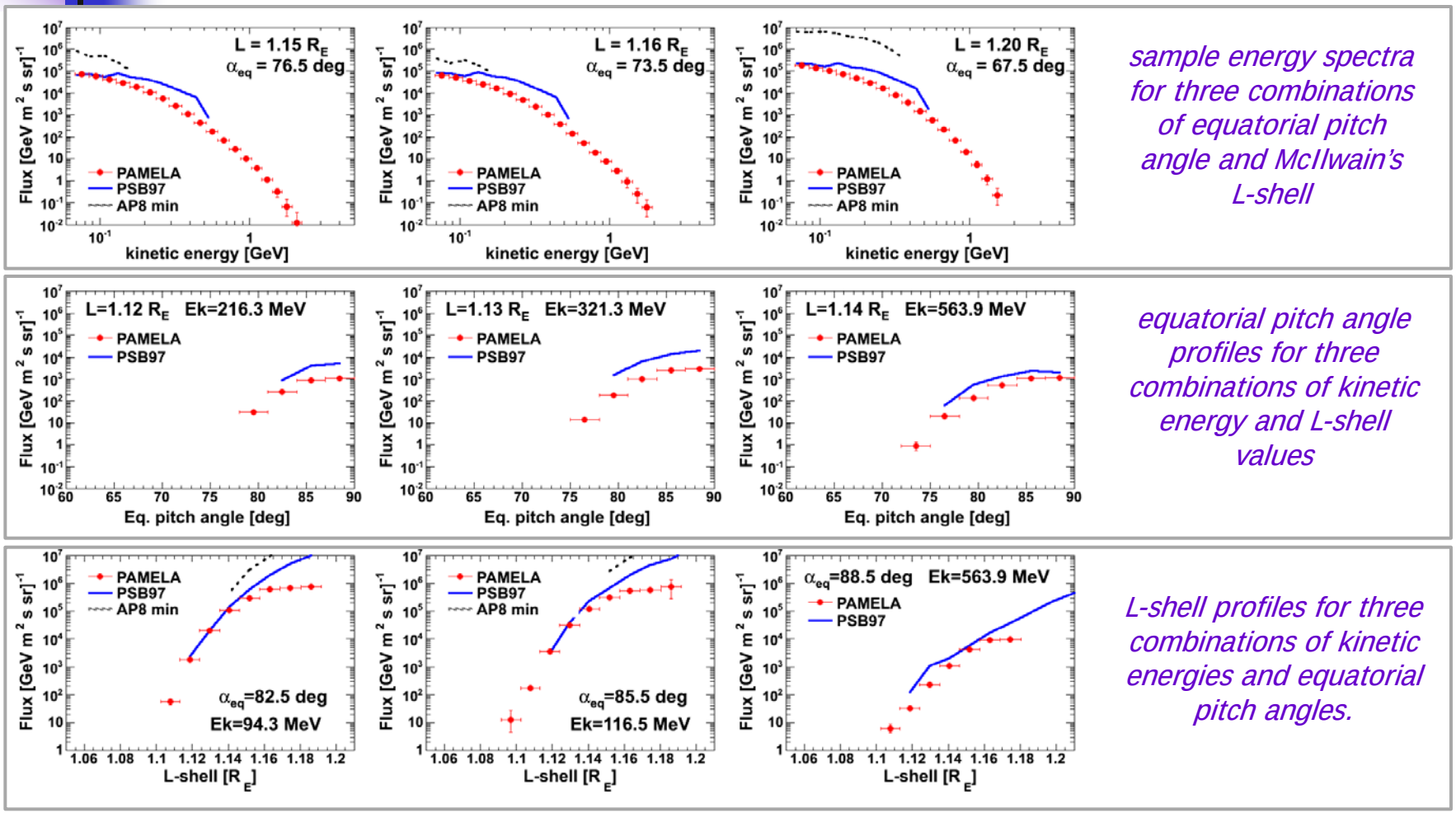

sample energy spectra for three combinations of equatorial pitch angle and McIlwain's L-shell

equatorial pitch angle profiles for three combinations of kinetic energy and L-shell values

L-shell profiles for three combinations of kinetic energies and equatorial pitch angles.

Stably-trapped differential fluxes ($GeV^{-1}m^{-2}s^{-1}sr^{-1}$) compared with predictions from **AP8-min** (Sawyer & Vette 1976) and **PSB97** (Heynderickx et al. 1999) semi-empirical models, denoted with dashed black line and the solid blue line respectively. Model calculations from the SPENVIS on-line system (Heynderickx et al. 2000).

Comparison with theoretical models

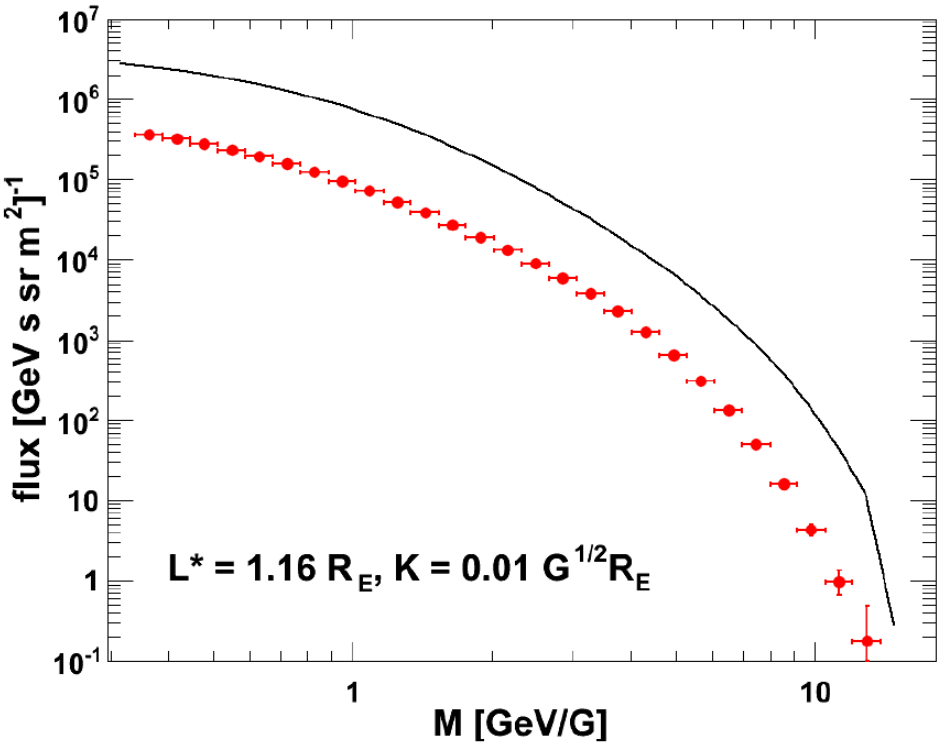

Stably-trapped differential flux ($GeV^{-1}m^{-2}s^{-1}sr^{-1}$) at geomagnetic equator compared with a theoretical calculation by Selesnick et al. (2007).

Spectra are reported as a function of first adiabatic invariant *M*, for sample values of *K* and *L** invariants.

Geomagnetically trapped antiprotons

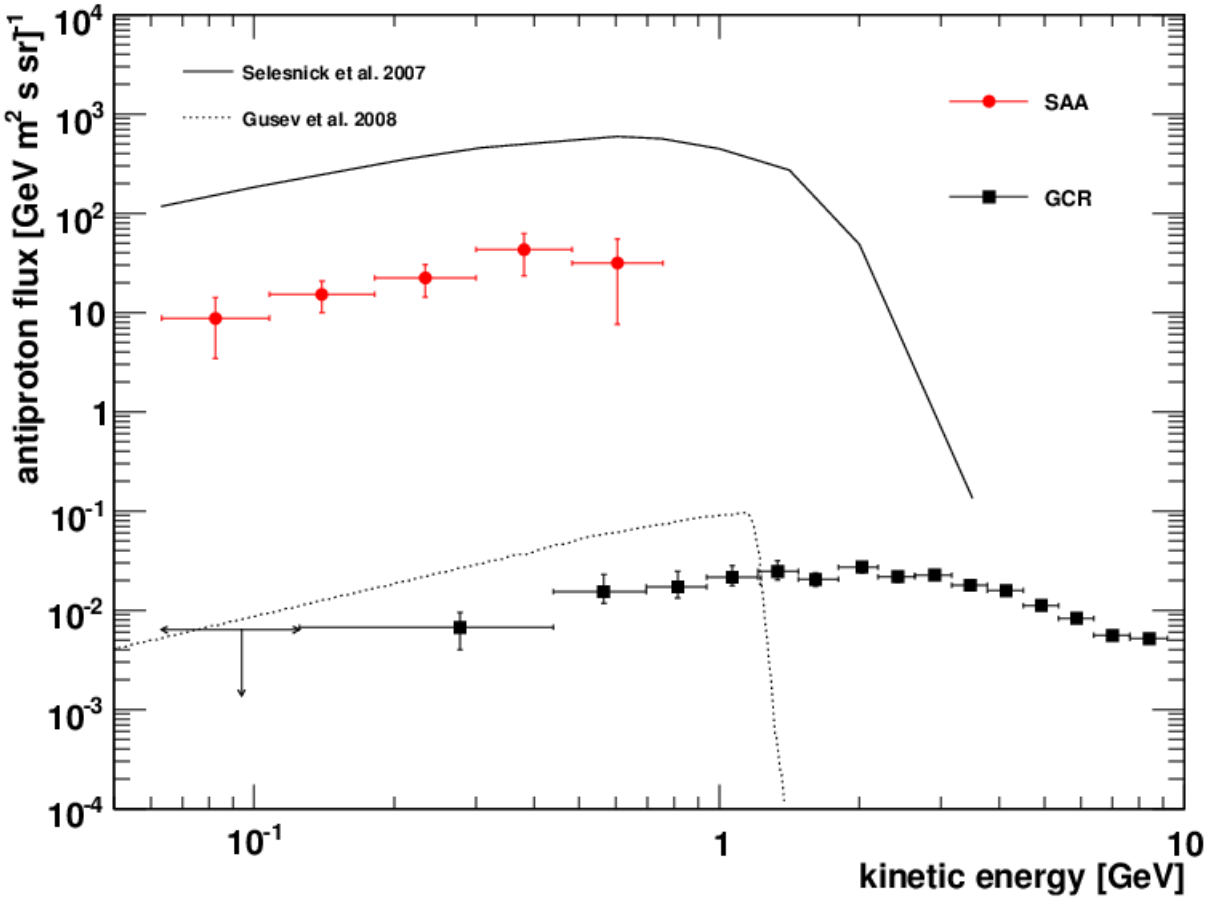

Adriani et al., *"The discovery of geomagnetically trapped cosmic-ray antiprotons"*, ApJ 737 L29, 2011

Re-entrant albedo protons

Particle classification

Based on particle trajectory tracing. By using combined selections on corresponding mean frequencies ω_i (i =gyro, bounce, drift) as a function of several variables of interest (E, α, Λ, etc.), the analyzed sample was sub-divided into two main categories:

1) events with trajectories similar to those of stably-trapped protons from the inner belt, but originated and re-absorbed by the atmosphere during a time shorter than a few drift periods, were identified as **quasi-trapped**. Their trajectories were verified to satisfy the adiabatic conditions, in particular the hierarchy of temporal scales:

$$\omega_{bounce}/\omega_{gyro} \leq 0.3 \text{ and } \omega_{drift}/\omega_{bounce} \leq 0.03$$

2) The rest of the sample was classified as **un-trapped**.
Qualitatively, two subcomponents can be identified:

   a) **precipitating protons**, with lifetimes shorter than a bounce period. Values of ω_{bounce} are similar to those of quasi-trapped protons, while ω_{gyro} distribution is much broader outside the SAA, extending to much lower values.

   b) **Pseudo-trapped protons**, with relatively long lifetimes. Non-adiabatic trajectories: large gyro-radii and ω_{drift}, and small ω_{gyro} and ω_{bounce} values, resulting in unstable trajectories due to resonances occurring between component frequencies. They can perform several drift cycles (up a few hundreds), sometimes forming intermediate loops, reaching large distances from the Earth's surface before they are re-absorbed by the atmosphere.

AACGM coordinates

- Data were analyzed in terms of “Altitude Adjusted Corrected Geomagnetic” (AACGM) coordinates, developed to provide a more realistic description of high latitude regions by accounting for the multipolar geomagnetic field.

- They are defined such that all points along a magnetic field line have the same geomagnetic latitude and longitude, so that they are conceptually closely related to invariant magnetic coordinates (Baker et al. 1989; Gustafsson et al. 1992; Heres & Bonito 2007).

- The reference frame is identical to standard “Corrected Geomagnetic Coordinates” (CGM) at the Earth’s surface.

Tracing results:
lifetime distributions

Lifetime = the time between the particle origin (traced backward) and its subsequent absorption (traced forward) in the atmosphere (i.e. the tracing time).

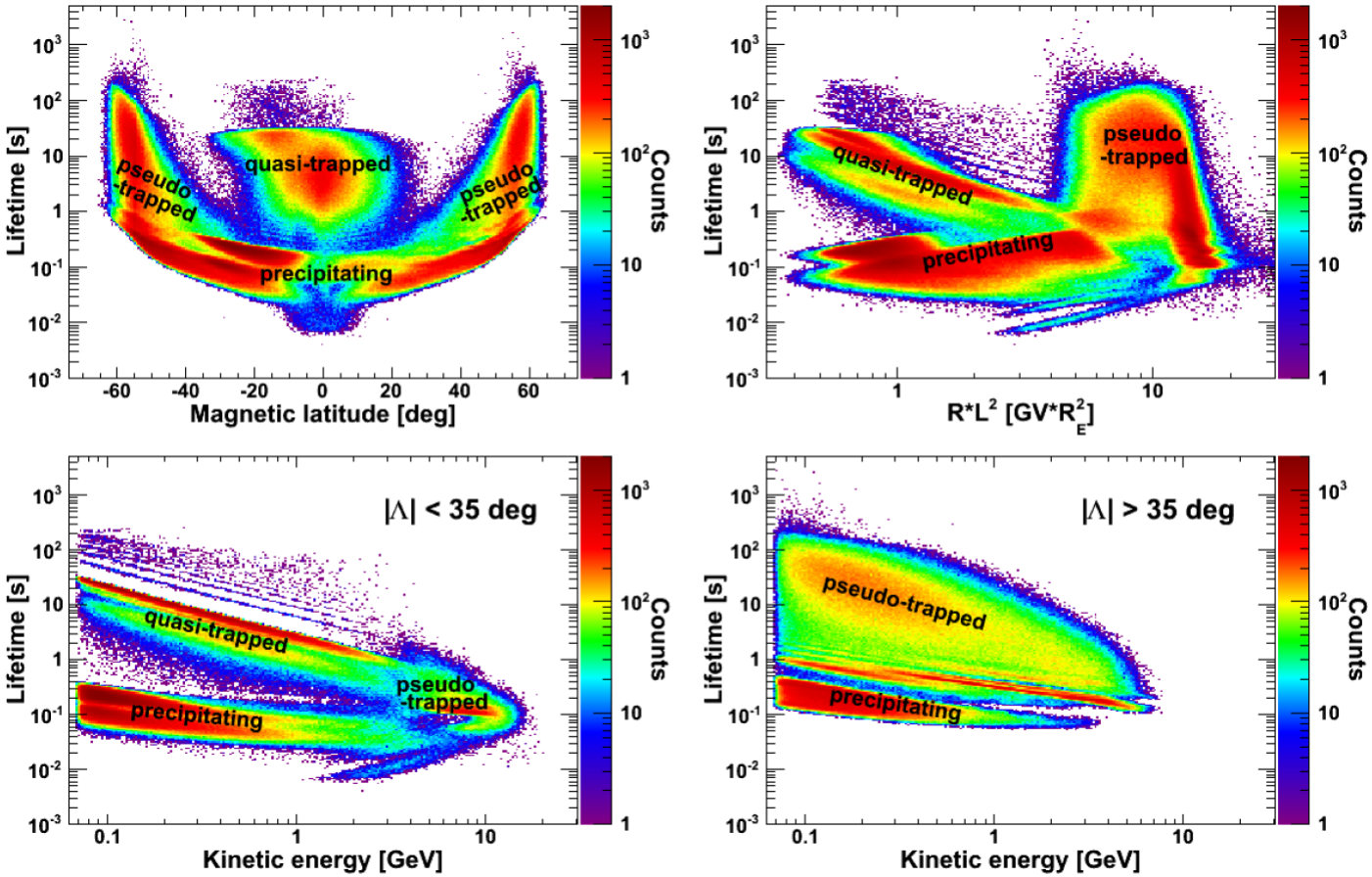

Lifetime distribution for the measured sample as a function of the geomagnetic latitude (top-left panel), of the product of rigidity and *L*-shell squared (top-right panel), and of kinetic energy (bottom panels, for geomagnetic latitudes lower and greater than 35 deg, respectively).

Tracing results:
origin / impact points

origin points | **impact points**

quasi-trapped

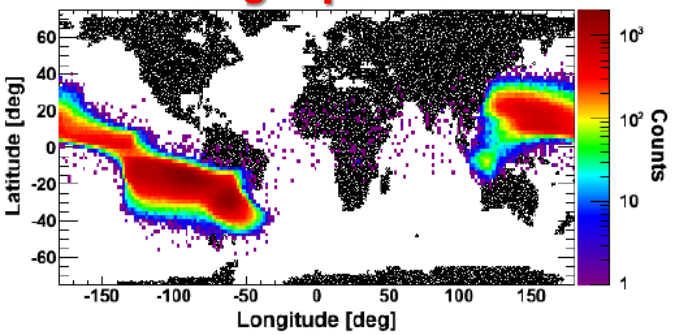

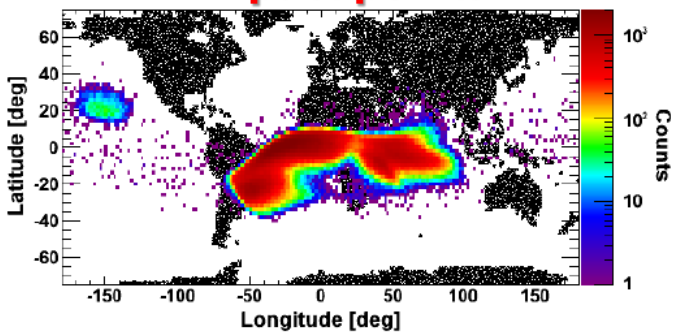

precipitating

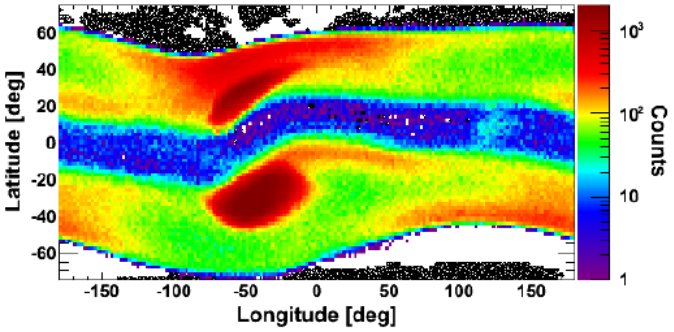

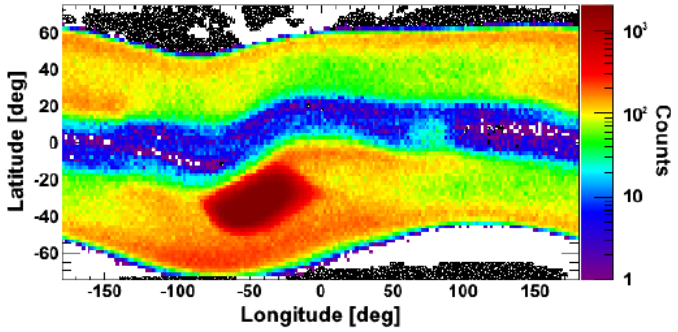

pseudo-trapped

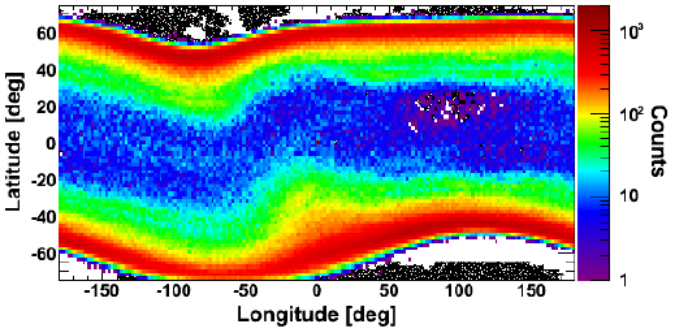

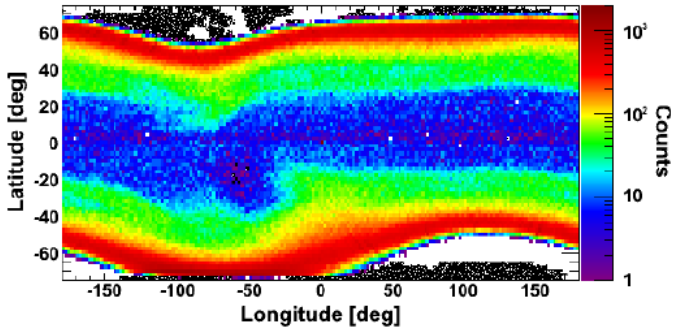

Count distributions of the production (left panels) and absorption (right panels) points on the atmosphere (40 km) as a function of the geographic coordinates.

Tracing results:
origin / impact points

- **Quasi-trapped**:
  - origin points are located in a region extending westward from the SAA.
  - While drifting from the SAA, protons encounter stronger magnetic fields and the altitude of their mirrors point increases, until they reach again weaker magnetic field regions;
  - then their mirroring altitude decreases and finally they are absorbed by the atmosphere, mainly on the region on the East side of the SAA.
  - Both production and absorption points are located in two regions, in the southern and in the northern magnetic hemisphere respectively, as a consequence of the multipole moment of the Earth's magnetic field.

- **Un-trapped**:
  - **Precipitating:**
    - since they are created and absorbed by the atmosphere in a very short time, their production and absorption points are located near the detection position, populating the whole geomagnetic region explored by PAMELA;
    - indeed, absorption points have a peak in the SAA, while origin points have an additional peak in the northern magnetic region corresponding to southern mirror points in the SAA.
  - **Pseudo-trapped:**
    - Similarly, production and absorption points for such a component spread over all longitudes.

Flux maps

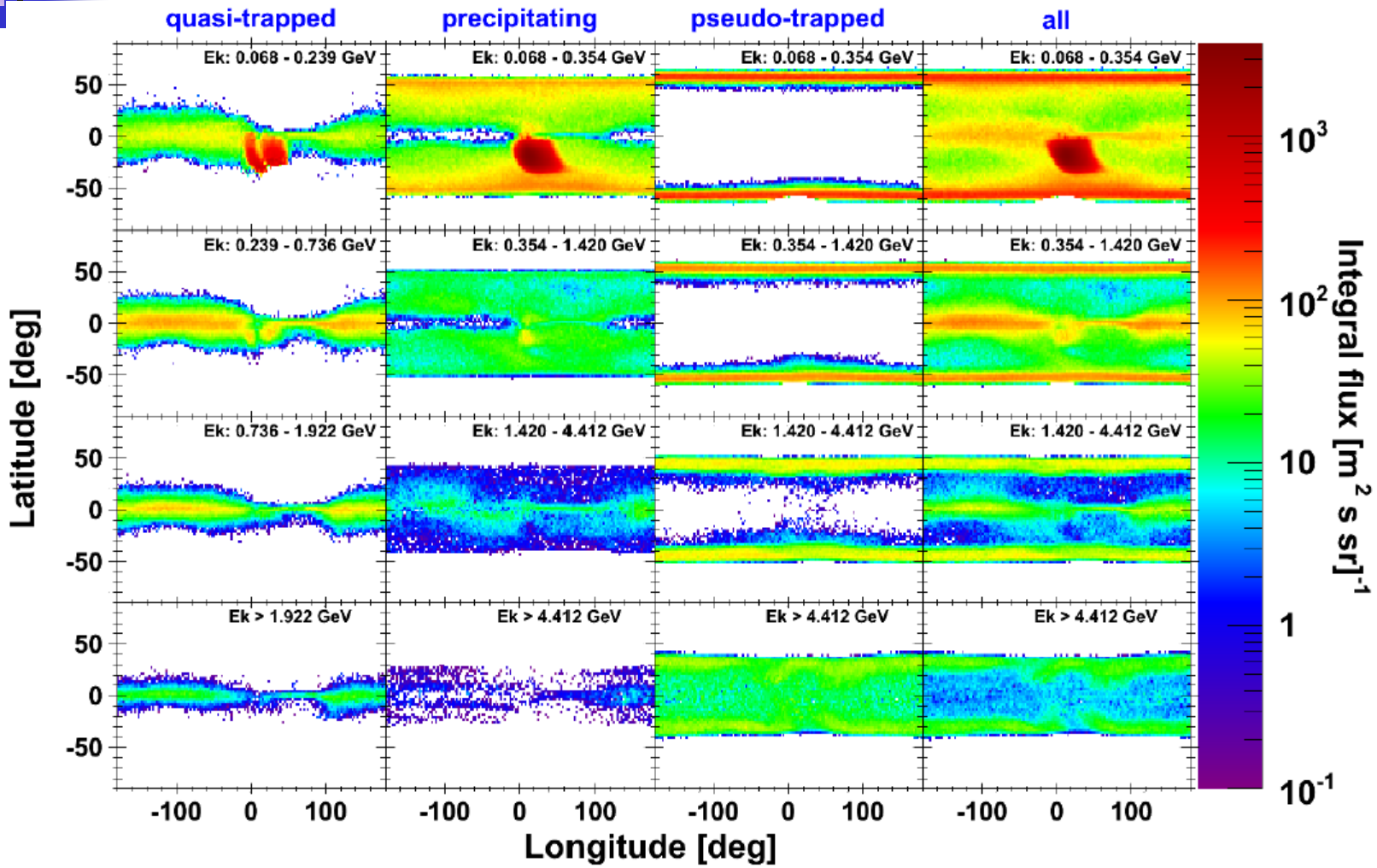

Under-cutoff proton integral fluxes ($m^{-2}s^{-1}sr^{-1}$) as a function of magnetic longitude and latitude, for different energy bins. Results for the several proton populations are reported (from left to right): quasi-trapped, precipitating, un-trapped and the total sample.

Energy spectra vs latitude

Differential energy spectra outside the SAA region measured for different bins of magnetic latitude (see the labels).

Results for the different proton populations are shown: quasi-trapped (**blue**), precipitating (**green**), pseudo-trapped (**red**) and interplanetary (**black**).

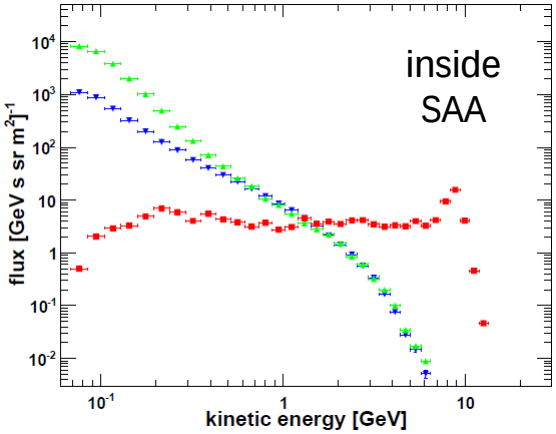

Differential energy spectra in the **SAA** region (B<0.23 G)

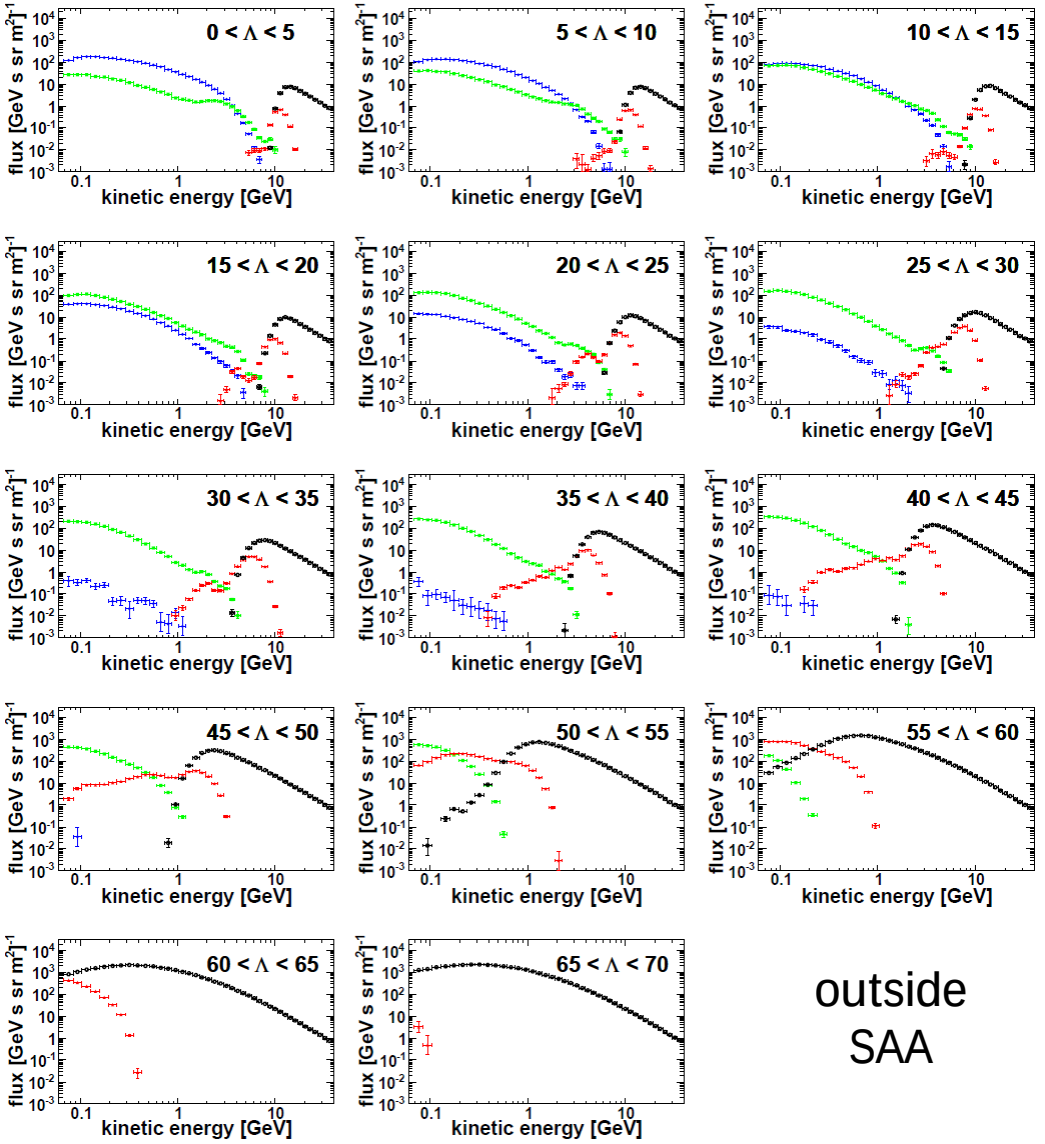

outside
SAA

Penumbra region

Penumbra: region where protons of both interplanetary and atmospheric origin are present

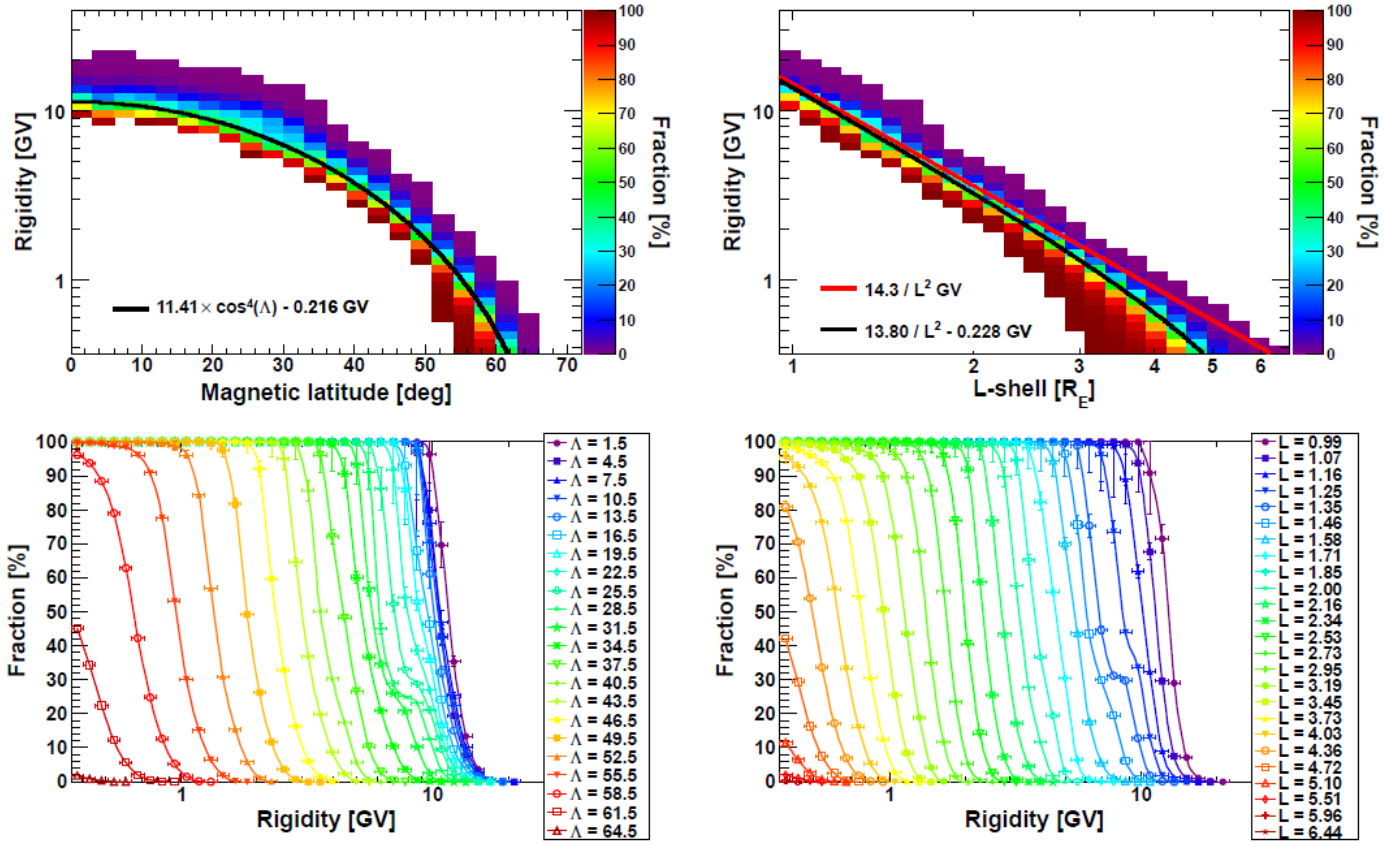

Top panels: fraction of albedo protons in the penumbra region, as a function of particle rigidity and magnetic latitude (left) and McIlwain's *L*-shell (right); black curves are a fit of points with equal percentages of interplanetary and albedo protons, while the red line denotes the Störmer vertical cutoff for the PAMELA epoch.
Bottom panels: corresponding rigidity profiles, for different values of magnetic latitude (left) and McIlwain's *L*-shell (right); values at bin center are reported in labels. Lines are to guide the eye.

Conclusions

- PAMELA measurement of energetic (> 70 MeV) protons of atmospheric origin at low Earth orbits (350-610 km) has been presented
  - data acquired by PAMELA between July 2006 and September 2009
  - analyzed according to the adiabatic theory of charged particle motion in the geomagnetic field
  - and classified into different (geomagnetically trapped, re-entrant albedo) components on the basis of trajectory behaviors in the magnetosphere evaluated with particle tracing techniques.

- PAMELA results improve the description of the **geomagnetically trapped proton radiation** at low altitudes (down to L~1.1 R_E) and at high energies (up to E~4 GeV), where current models suffer from large uncertainties.

- ✓ PAMELA measurements provide important information on trapping and interaction processes in the geomagnetic field, and also enhance the description of **re-entrant albedo** protons (quasi-trapped, short- and long-lived un-trapped) in different regions of the magnetosphere, including the penumbra.

- Future work
  - Analysis of data acquired by PAMELA after September 2009
  - Analysis of electrons, positrons and light nuclei
  - Development of a **PAMELA model** for the high-energy radiation at low Earth orbits

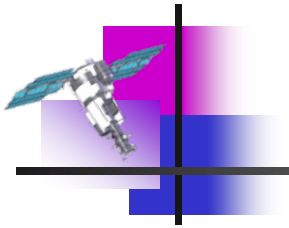


PaMeLa

Comparison with AMS-01

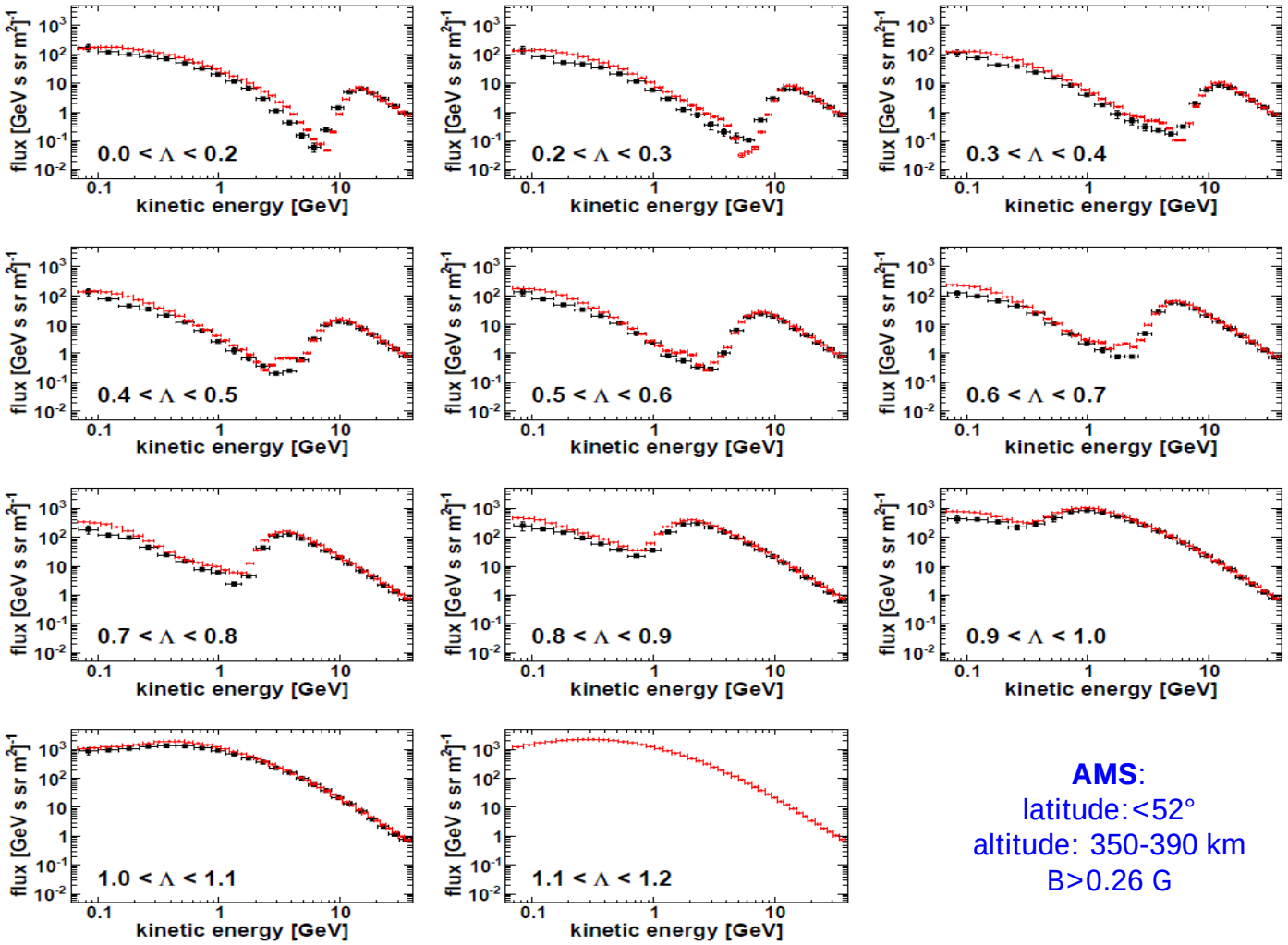

AMS:
latitude:<52°
altitude: 350-390 km
B>0.26 G

Comparison between PAMELA (**red**) and AMS-01 (Alcaraz et al. 2000) (**black**) proton spectra, for different bins of geomagnetic latitudes (radians). Reported fluxes include both interplanetary and under-cutoff components.